







This paper proposes a new monitoring system model utilized to predict the next state of moving agent(s) in a closed space as in Fig.1 by fusing information from multiple sensors of different types.

The area under surveillance is divided into four zones A, B, C and D shown in Fig.1 where each is only a ring with a width that is wide enough to be completely covered by the sonar sensor's cone's diameter. This sensor could be mounted in the middle of the ceiling of each ring and rotating at a fixed scanning speed to cover the whole ring and be able to provide a total number of agents at any given time in any zone [6, 7]. As shown in Fig.2 the model also reads in data from a grid of laser sensors [6, 8, 9] to capture agent speed. The following laser sensor network was assumed; four sensors in the X direction and another set of four laser sensors in the Y direction with each of them reporting the agent(s) speed in feet per second as in Fig.2.

Finally an identification data transmitter is associated with each agent and captured by RF Radio Frequency sensor [10, 11] to support the system with an ID of any moving agent. For sake of simplicity, radio frequency sensor will provide three pre-defined types of agent's access rights ("Trusted", "Semi-Trusted" and "Unknown"). Laser and sonar sensor data sets will then be fed into a sensor similarity processing sub-system that will be responsible to filter out any noisy sensor input of each sensor-type and come up with a single reading based on sensor similarity method. After sensor data have been filtered, speed on X-axis and Y-axis outputs will be processed in a state estimation and transformation.

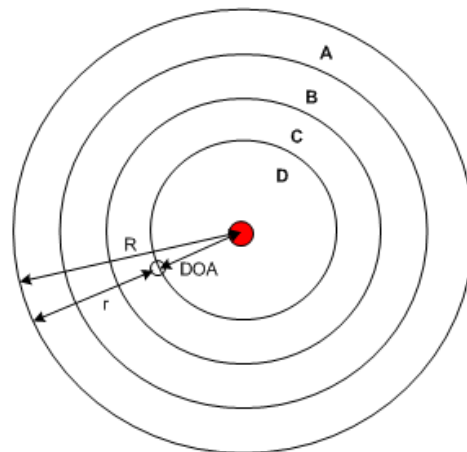


Figure 1. Security monitoring system space with the red circle denotes the valuable asset.

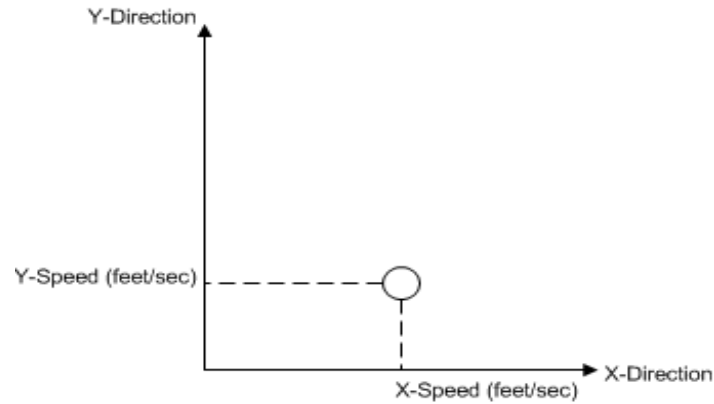


Figure 2. Agent speed captured on X and Y direction.

Finally sensor complementarity stage starts where sensor data fusion/complementarity is performed using type-2 fuzzy logic inference system to produce a suspiciousness decision for each moving agent as shown in Fig.3.

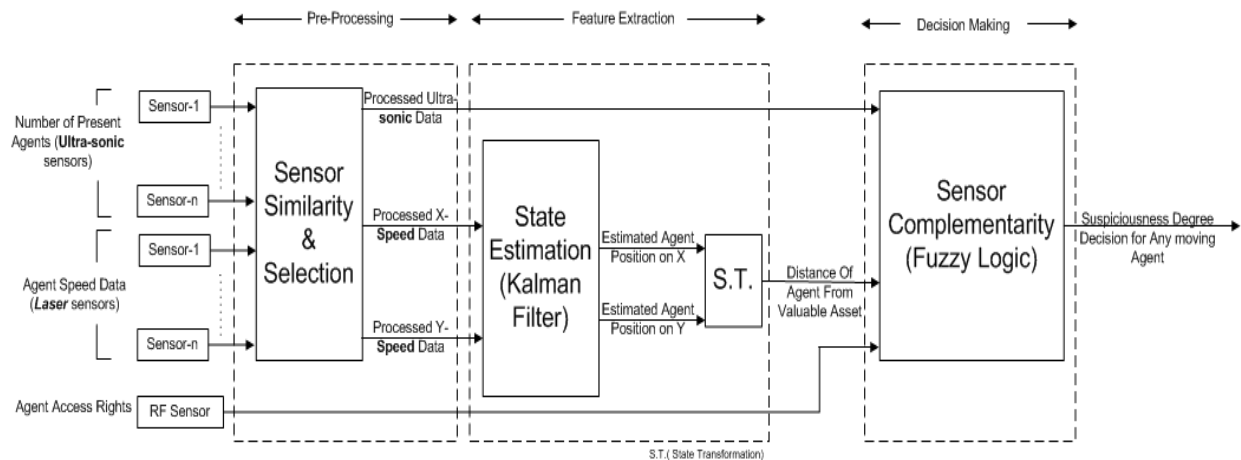


Figure 3. Security System Block Diagram.

#### IV. SENSOR SIMILARITY AND SELECTION

Considering raw sensor measurements directly into sensor fusion may affect quality of fusion which leads to making wrong decisions in some cases where these measurements contain noisy and inaccurate data. Thus, pre-processing of these sensors plays an important role in sensor fusion. Only reliable subsets of the sensors are needed; subsets that are consistent and accurate.

In our proposed system data is collected from a total of eight different laser sensors mounted on the X-axis and on the Y-axis (four sensors on each axis) with each sensor having different standard deviation and mean. This paper proposes a new method of sensor similarity that utilizes

the concepts of relative closeness of sensors with respect to each other. Over all mechanism of sensor similarity is summarized in Fig.4.

Sensors closeness in measurement between sensors is defined as the distance of sensor “j” with respect to other sensors on the same axis to be:

$$d_j = (Max(j)_{pos} - GA_{mean}) / \sigma_j^2 \quad (1)$$

where  $GA_{mean}$  is the Global Arithmetic mean of all sensors (on a given axis) and  $Max(j)_{pos}$  is the best estimate of the true state of sensor “j” for data collected over one second time span sensor readings that are closest to the true state and defined as:

$$Max(j)_{pos} = Max[Posteriori(\hat{x}_j)] \quad (2)$$

where Posteriori of  $j^{th}$  sensor’s reading given the observation  $x_j$  is  $P(s_j|x_j)$ .



Figure 4. Flow chart shows how sensor similarity is performed.

a. Iterative Bayes estimate and Maximum Posteriori

In this estimate the posterior of the different sensors was obtained based on Bayes formula:

$$p(s|x) = \frac{p(x|s)p(s)}{p(x)} \quad (3)$$

Where “s” is the state and “x” is the observation. The probability of “s” given the observation “x”; the observation drawn from normal distribution  $N(\mu, \sigma^2)$  where  $\mu$  is the mean and standard deviation, so the mean of the likelihood function is the state under consideration which is represented as:

$$p(x|s) = \frac{1}{\sigma\sqrt{2\pi}} e^{\left(\frac{-(x-s)^2}{2\sigma^2}\right)} \quad (4)$$

and:

$$p(x) = \frac{1}{\sigma\sqrt{2\pi}} e^{\left(\frac{-(x-\mu)^2}{2\sigma^2}\right)} \quad (5)$$

The only unknown term left in Bayes is  $P(x)$ . We know that:

$$\sum p(s|x) = 1 \quad (6)$$

so:

$$\sum \frac{p(x|s)p(s)}{p(x)} = 1 \quad (7)$$

then:

$$p(x) = \sum p(x|s)p(s) \quad (8)$$

The right side of equation (8) is computed for all observations and then divide by the total sum of these values to compute  $P(x|s)$ . This process was made iterative as more observations arrive by setting the priori  $P_r(i+1) = \text{Posteriori}$  of the previous observation  $P_o(i)$  and the maximum posteriori is pulled out at each iteration.

## b. Global and Local Arithmetic Means

In this paper, the  $LA_{mean}$  is defined to be the Local Arithmetic Mean [12] for each sensor over its  $k$  observations and defined as:

$$LA_{mean} = (1/k) \sum_{i=1}^k x_i \quad (9)$$

and  $GA_{mean}$  in equation (1) to be the mean of all sensor local arithmetic means that is defined as follows:

$$GA_{mean} = \frac{\sum_{n=1}^4 LA_{mean}}{n} \quad (10)$$

where  $n$ : is the number of used sensors for an axis ( $n = 4$  in our example) and finally, in equation (1) refers to the standard deviation of the sensor “ $j$ ” given the fact that each sensor has a different mean and standard deviation.

After each sensor’s  $d_j$  is calculated it is compared to a pre-defined threshold distance  $d_{th}$  to determine if the reading of this sensor should be rejected or considered which constitutes the part of sensor selection. In this paper we assume threshold  $d_{th}$  is concluded from a previously conducted calibration of the sensor network.

If the sensor’s reading is considered then it is factored in when calculating the overall average of all considered readings:

$$Total_{average} = \frac{\sum_{i=1}^n LA_{mean_i}}{n} \quad (11)$$

where “ $n$ ” here is the total number of accepted sensors.

Finally, a single reading as a similarity output is obtained. This algorithm of similarity is applied to laser sensors on both X axis and Y axis, and to the sonar sensors as well.

## V. STATE ESTIMATION AND TRANSFORMATION

### a. Kalman Filter

The method of Kalman filtering is a widely utilized for filtering sensor measurement data and for sensor data fusion as well [13].

Kalman filter uses measurements that are observed over time that contain noise, and produces values that tend to be closer to the true values of the measurements and their associated calculated values. The Kalman filter is a set of mathematical equations that provides an efficient computational (recursive) means to estimate the state of a process, in a way that minimizes the mean of the squared error. Kalman filtering is an ongoing cycle of time updating that projects the current state estimate ahead in time and the measurement updating that adjusts the projected



estimate by an actual measurement at that time. The equations for those two updates are presented below [14]:

The first step is the Prediction (Discrete KF time update):

(1) Project the state ahead:

$$\hat{x}_k = A_k \hat{x}_{k-1} + B_k u_k + w_k \quad (12)$$

Where  $x_k$  is the state vector (agent's position and velocity),  $A_k$  is the state transition model that is applied to the previous state  $x_{k-1}$ ,  $B_k$  is the control input model that is applied to the control vector  $u_k$  and  $w_k$  is the process noise that is assumed to be drawn from a zero mean normal distribution with covariance  $Q$ .

$$p(w) \sim N(0, Q) \quad (13)$$

(2) Project the error covariance ahead:

$$P_k^- = A_k P_{k-1} A_k^T + Q \quad (14)$$

The second step is the Update (Discrete KF measurement update):

(1) Compute the KF gain:

$$K_k = P_k^- H^T (H P_k^- H^T + R)^{-1} \quad (15)$$

Where  $H$  is the measurement vector of the measurement  $z_k$  of the true state space:

$$z_k = H_k x_k + v_k \quad (16)$$

$v_k$  is the measurement noise that is assumed to be drawn from a zero mean normal distribution with covariance  $R$ .

(2) Update estimate with measurement  $z_k$ :

$$\hat{x}_k = \hat{x}_k^- + K_k (z_k - H \hat{x}_k^-) \quad (17)$$

(3) Update the error covariance:

$$P_k = (1 - K_k H) P_k^- \quad (18)$$

For application purposes, estimates of the agent's position on the X and the Y axes of the space are needed. Kalman Filter was chosen to accomplish this task.

A system state was defined in this case to be the position and the speed.

$$V_x = X\_Total_{average} \quad (19)$$

$$V_y = Y\_Total_{average} \quad (20)$$

where the agent's speed at the X-axis is the final  $X\_Total_{average}$  that was arrived at. After collecting agent's data on X axis and deriving its corresponding position data as (same applies for the Y axis):

$$P_x = t * X\_Total_{average} \quad (21)$$

$$P_y = t * Y\_Total_{average} \quad (22)$$

Where, t is the time.

Kalman filter was applied on our system to estimate agent's next position.

#### b. State Transformation (Homogeneous Sensor Complementarity)

Multi-sensor complementarity is the synergistic use of the information provided by different sensory devices to assist in the accomplishment of a system task.

It refers to any stage in the integration process where there is an actual combination of different sources of sensory information into one sensory representation [15]. Sensor complementarities or correlation is especially advantageous when heterogeneous sensors are employed because of the potential to aggregate different views of the same incident.

For our application we are interested in the distance of an agent (DoA) from the valuable asset under surveillance; thus a transfer of the system state (agent's position on X and Y axes) to another form is needed where it describes the agent's distance with respect to asset. Since the agent could be moving in any direction in the space (its motion angle from asset will always change) we are always interested in that continuously changing distance. Therefore, we need to transform the X and Y to  $r$  and  $\theta$  (Cartesian to polar). This is defined as homogeneous sensor complementarity as the system used reading from multiple sensors of the same type (speed on X and speed on Y). However, the system will only utilize the  $r$  (radial distance) part of that information then DoA is easily calculated to be  $R-r$ ; where R is the radius of the largest circle where the agent is first detected by the sensors (Fig.1).

## VI. DECISION MAKING/TYPE-2 FUZZY (HETREGONEOUS SENSOR COMPLIMENTARITY)

The last part of this proposed system is the security decision making which utilizes the previous sub-system output to make a decision using an interval type-2 fuzzy system since it is suitable to make a precise decision in uncertain circumstances.

a. Interval Type-2 Fuzzy Inference System

Unlike a type-1 set where the membership grade is a crisp value in [0, 1], a type-2 fuzzy set shown in Fig.5 is characterized by a fuzzy membership function, where the membership of each point of this set is a fuzzy set in [0, 1] [16].

An Interval type-2 fuzzy set makes room for non-deterministic truth degree and uncertainty [17, 18] (foot print of uncertainty FOU shown in Fig.5) for an element that belongs to a set. A type-2 fuzzy set denoted by,  $\tilde{A}$ , is characterized by a type-2 membership function,  $\mu_{\tilde{A}}(x,u)$ , where  $x \in X$ ,  $u \in J_x^u \subseteq [0,1]$  and  $0 \leq \mu_{\tilde{A}}(x,u) \leq 1$ .

$$(\tilde{A}) = \{(x, \mu_{\tilde{A}}(x)) \mid x \in X\} \tag{23}$$

$$(\tilde{A}) = \{(x, u, \mu_{\tilde{A}}(x, u)) \mid \forall x \in X, \forall u \in J_x^u \subseteq [0,1]\} \tag{24}$$

It is the bounded area in Fig.5 and mathematically it is the union of the upper and lower membership functions [15, 19], where the upper and lower memberships are Gaussian functions:

$$Upper(FOU(\tilde{A})) = N(m, \sigma_2; x) \tag{25}$$

$$Lower(FOU(\tilde{A})) = N(m, \sigma_1; x) \tag{26}$$

Where;  $\sigma_1$  and  $\sigma_2$  are the standard deviations for lower and upper membership functions respectively and  $m$  is the mean of both.

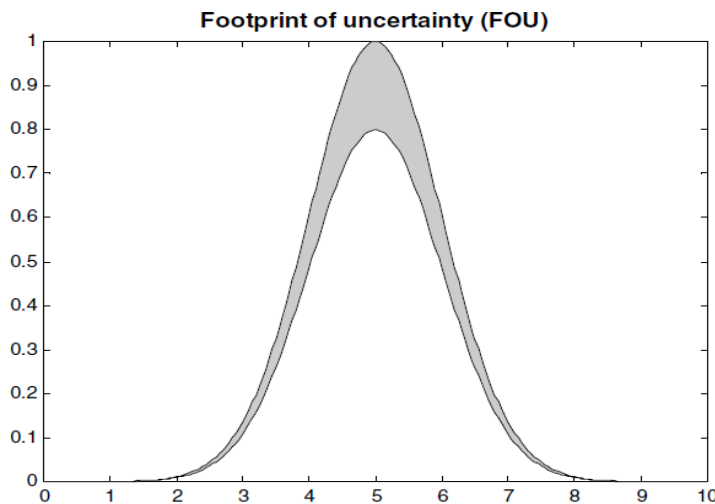


Figure 5. A Foot print of uncertainty of a sample interval type-2 Gaussian membership function.

b. Heterogeneous Sensor Complementarity

In this paper a decision making sub-system (an interval type-2 fuzzy logic system) is defined to be the heterogeneous sensor [19] complementarity as it reads in three different sensor data types and generates a fourth type of data that is totally different from the input ones. It is heterogeneous because it will generate a percentage output (percentage data type output) based on the number of agents (NoA that is different data type) and their relative distances from the valuable asset at any given time, the distance of agents (DoA that is a different data type) and finally, the agent's access rights (That is also different data type input).

The first input which is the "Number of Agents" (NoA) is considered an input with four different fuzzy ranges. Ranges are "Low" indicating the total number of objects is in the low scale of the alarming system, a "Medium Low" is the next level up, "Medium High" is the second highest level and finally "High" is the highest possible level. The second input is  $DoA_f$  that is generated as:

$$DoA_f = DoA * f \quad (27)$$

Where (DoA) "Distance of Agent" from the asset in feet. DoA is categorized into four different fuzzy categories, "Agent is extremely close", "Agent is very close", "Agent is close" and "Agent is far" (Fig.1). Also, where "f" is a multiplication factor that is based on the "Access Rights" of any moving agent and defined to be twenty for a "Trusted" (denoted by "T"), ten for "Semi-Trusted" (denoted by "ST") and finally a one for an "Unknown" agent (denoted by "U"). Fig. 6 shows the type-2 fuzzy logic membership functions for both Number of Agents and Distance of Agents.

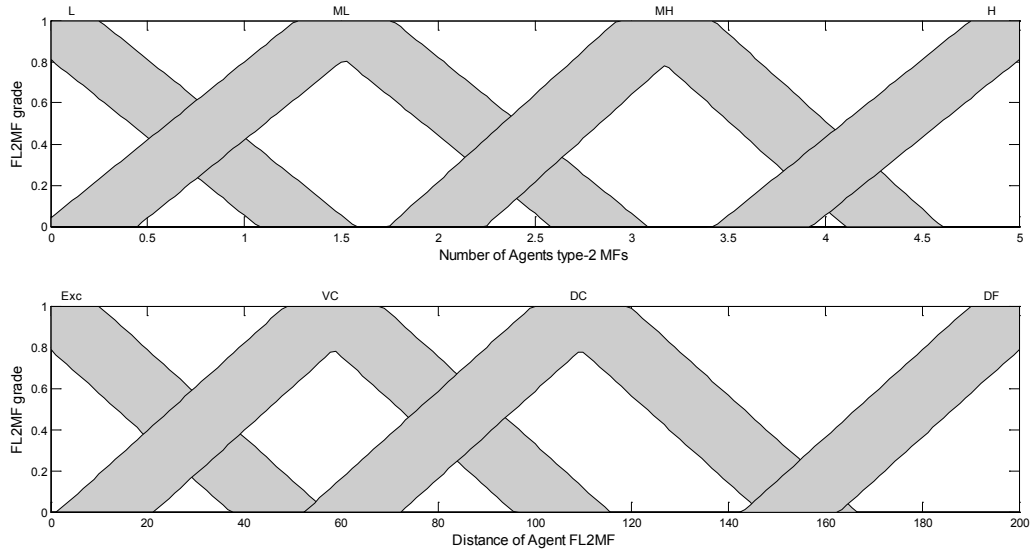


Figure 6. Interval type-2 Trapezoidal Membership functions for NoA and DoA respectively.

This was accomplished by setting a set of fuzzy inference system (FIS) rules (Fig. 7). Below is a sample of such rules:

If “Number of Agents” (NoA) is *High* and “Distance of Agent” (DoA) is *Extremely Close*  
 Then  
 “Degree of Suspiciousness” (DoS) is *Extremely Suspicious*

The proposed system has only one output which is the “Degree of suspiciousness” (DoS). This DoS is categorized into five levels of suspiciousness, “Not suspicious”, “Almost Suspicious”, “Suspicious”, “Very Suspicious”, and “Extremely suspicious” as shown in Fig.8 and is driven by the DoA<sub>f</sub> and NoA inputs [6, 20].

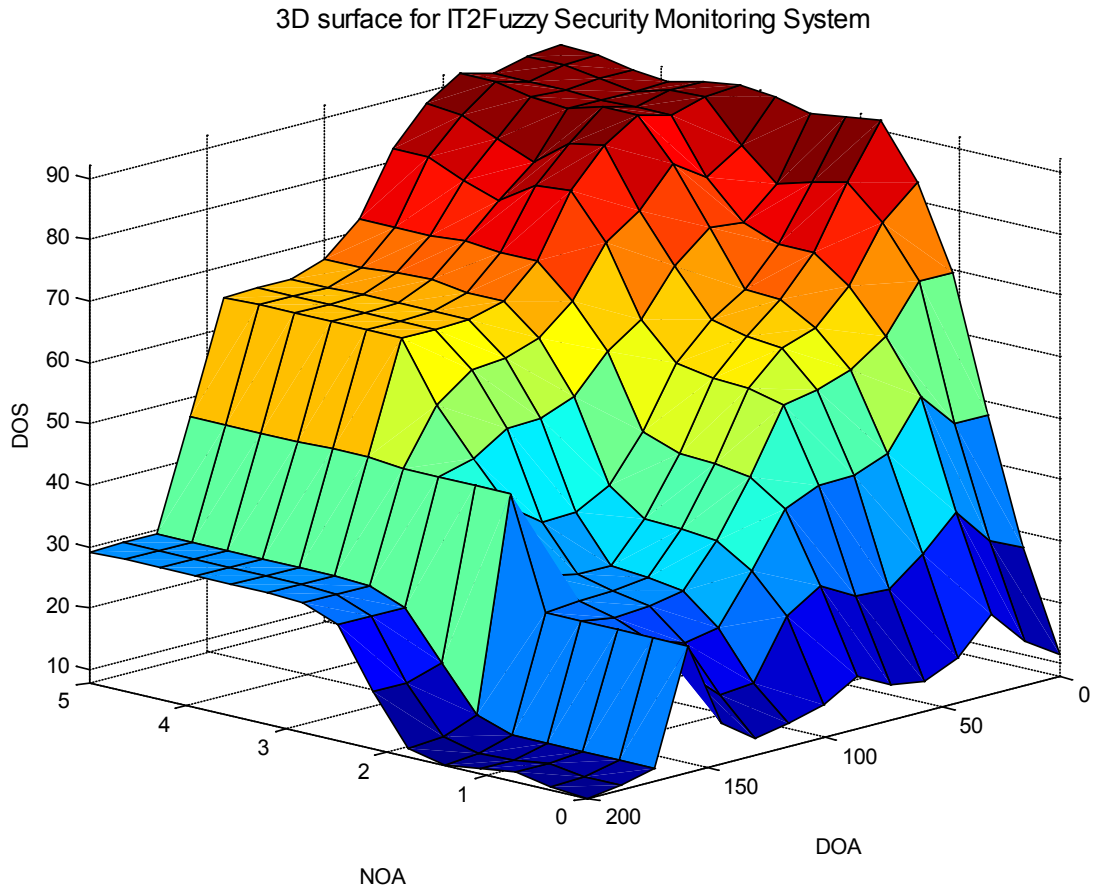


Figure 7. Interval type-2 Decision Surface Generated by FIS Rules.

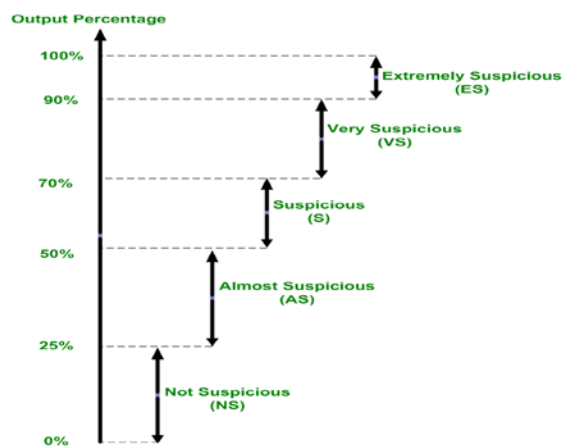


Figure 8. System Suspiciousness levels

## VII. RESULTS AND DISCUSSION

In this paper a realistic simulation of several scenarios of agents moving linearly were investigated. Evaluation for a single agent is shown here. Assuming agent's true speed is 3 feet/sec on X-axis the grid of four sensors (each sensor is slightly different from the other in its mean and standard deviation) captured this speed over one second time frame. Fig.7 shows agent speed captured by four sensors.

Sensor 1 of this group is assumed to be noisier with mean and standard deviation well distant from the other three. It was also assumed the agent's true speed is 5 feet/sec on Y-axis, the grid of four sensors (each sensor is slightly different from the other in its mean and standard deviation) on this axis also captured this speed over same time interval that is 1 second Fig.8 shows this agent's data on the Y-axis. Sensor 2 of this group is assumed to be the noisy sensor.

Local Arithmetic means were next computed for each the four sensors on X-axis over for measurement over one second are shown in Fig.9 and Fig.10 shows their equivalents on the Y-axis for the same time span. The next step in our sensor similarity is to compute the maximum posteriori for each of the X-axis sensors which is displayed in Fig.11 and compute those posteriori for the Y-axis as well as shown in Fig.12. After sensor similarity is applied for both sets of laser sensors (X and Y axes), a distance for each sensor was calculated and compared to a pre-defined threshold values that are 0.5 and 0.9 for X and Y respectively.

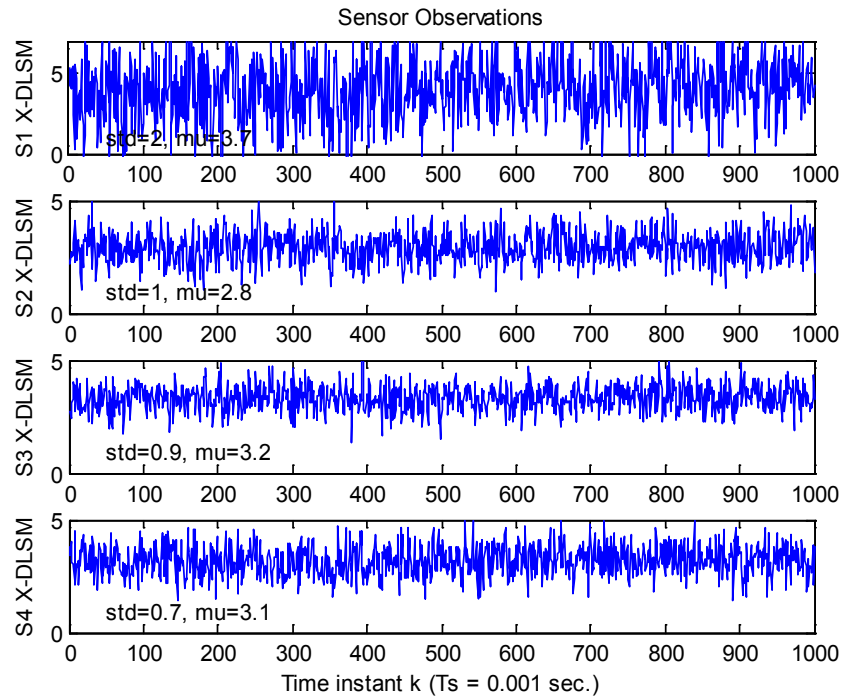


Figure 7. Speed data read by four Laser sensors on the X-axis of the sensor grid (where DLSM is Direction Laser Speed Measurement) and the number prefix refers to the sensor index in the grid.

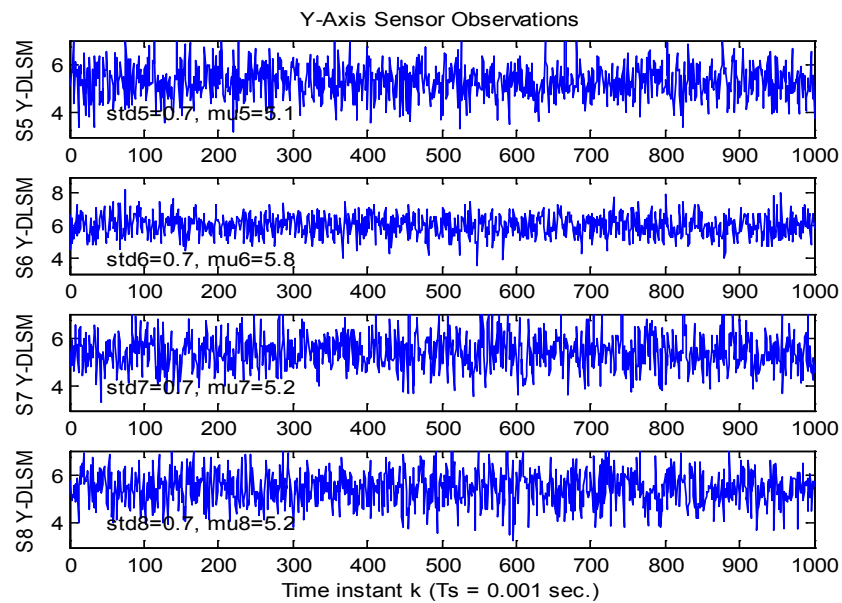


Figure 8. Speed data read by four Laser sensors on the X-axis of the sensor grid (where DLSM is Direction Laser Speed Measurement) and the number prefix refers to the sensor index in the grid



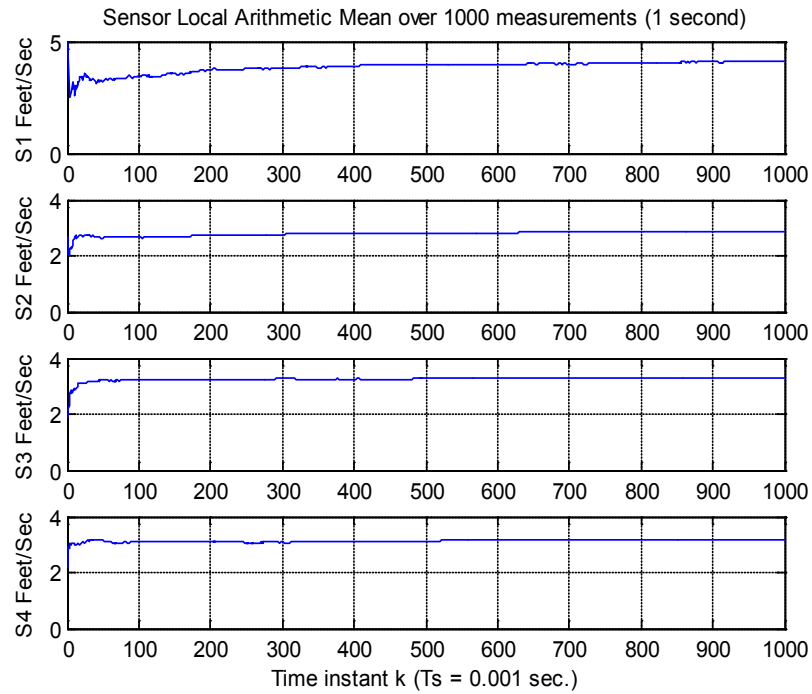


Figure 9. Local arithmetic mean (LAmean) for the four sensors on the X-axis over 1 second time span

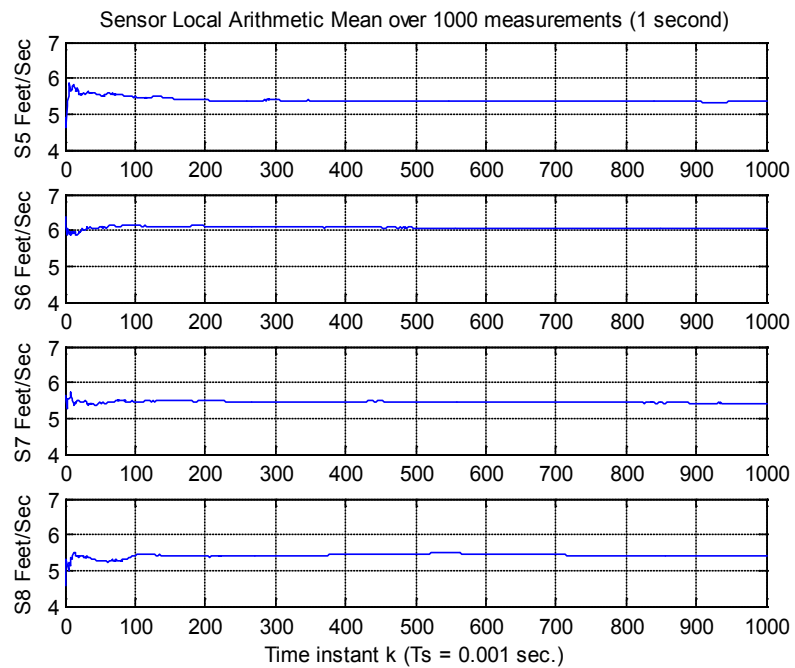


Figure 10. Local arithmetic mean (LAmean) for the four sensors on the Y-axis over 1 second time span

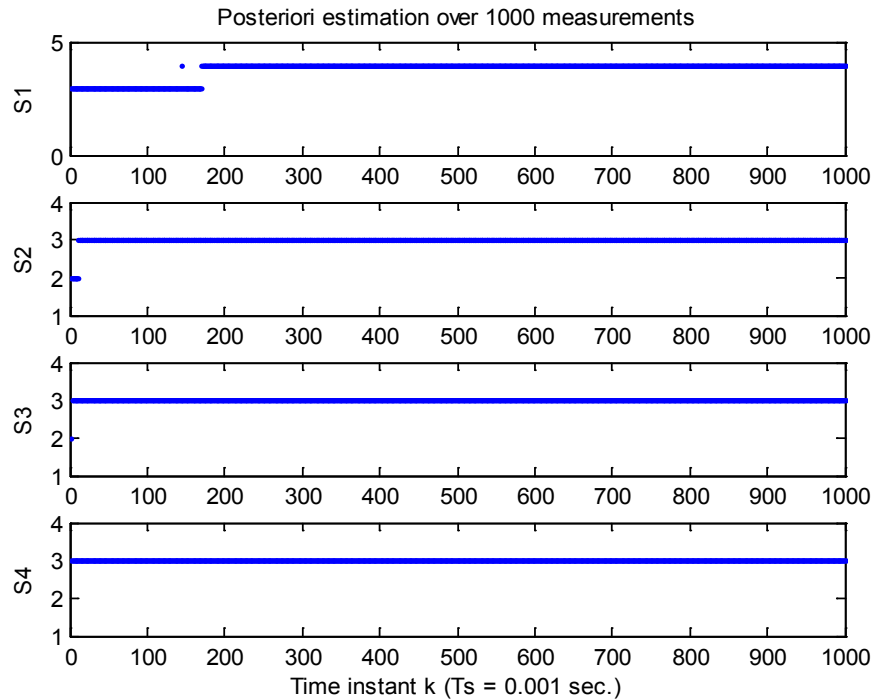


Figure 11. Max. Posteriori (Max(j)pos) for the four sensors on the X-axis over 1 second time span

Those thresholds are assumed to be based on sensor calibration data for each axis. New global arithmetic mean ( $Total_{average}$ ) was computed but based on only accepted sensors. Next Kalman filter was used to estimate agent's next state (next accumulated distance) on both axes based on the  $X_{Total_{average}}$  and  $Y_{Total_{average}}$  that are shown in Fig.13 and Fig.14 respectively.

State estimation (S.T.) that is the second to last block in our security system is then utilized to transform the distance data on (x, y) coordinates to (r,  $\theta$ ) polar coordinates (homogeneous sensor complementarity) as in Fig.15.

Finally, a weighing is applied to this computed  $r$  (based on its access right that is chosen to be 1.3 and 1.1 for "Trusted" and "Semi-Trusted" respectively and 1 for "Unknown"). Then it is fed to the decision making system to decide on its suspiciousness degree at any time during its movement shown in Fig.16. This figure displays evaluation two agents having the same speed values but different access rights ("Trusted" and "Unknown").

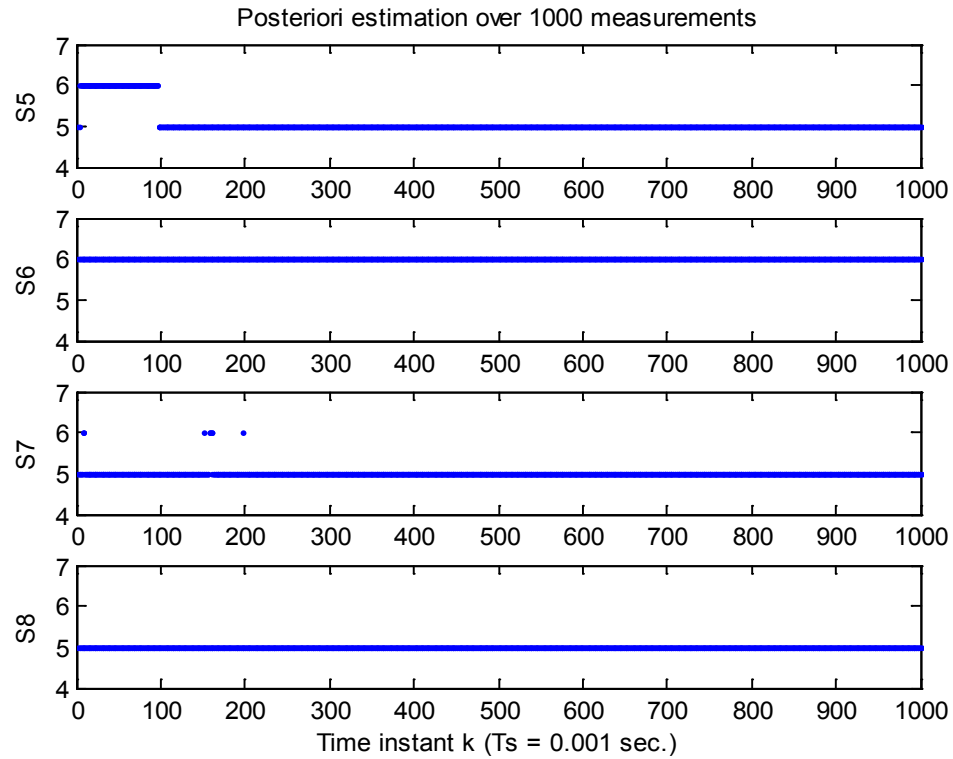


Figure 12. Max. Posteriori (Max(j)pos) for the four sensors on the Y-axis over 1 second time span

Fig.16 shows how the proposed security system was able to limit the DoS for the “Trusted” agent to less than 55%. However, it gave the “Unknown” agent almost a 65% for the same speed and distance accumulated values. It was shown that our system can actually use normal sensor data to filter it, estimate state, transform state and make a decision.

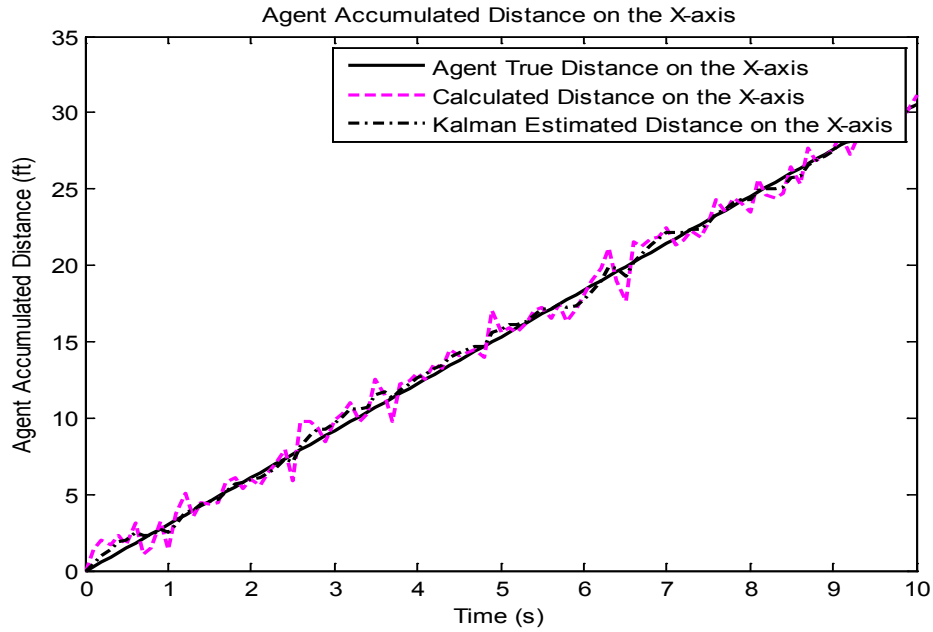


Figure 13. Agent position on X axis where “0” is the point where agent was first detected

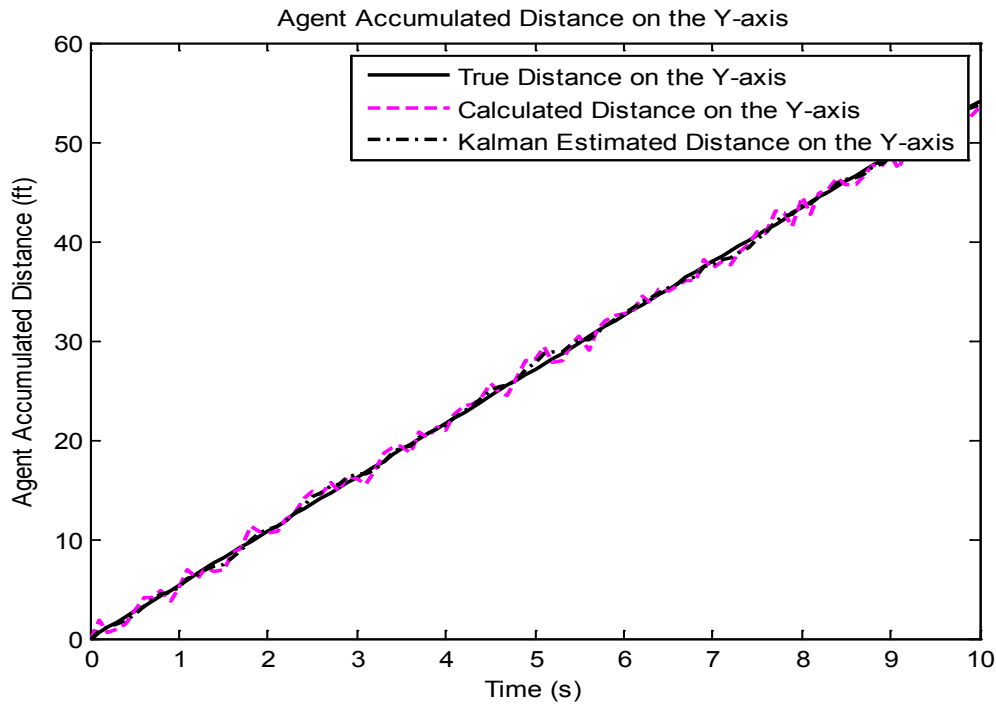


Figure 14. Agent position on Y axis where “0” is the point where agent was first detected

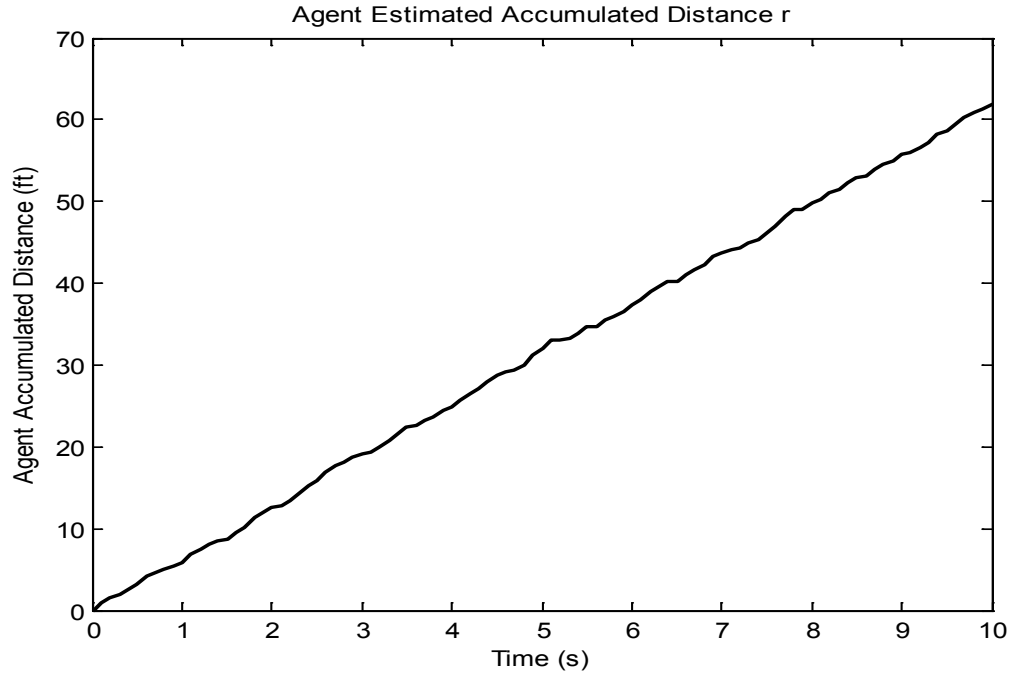


Figure 15. Agent accumulated distance in polar coordinates

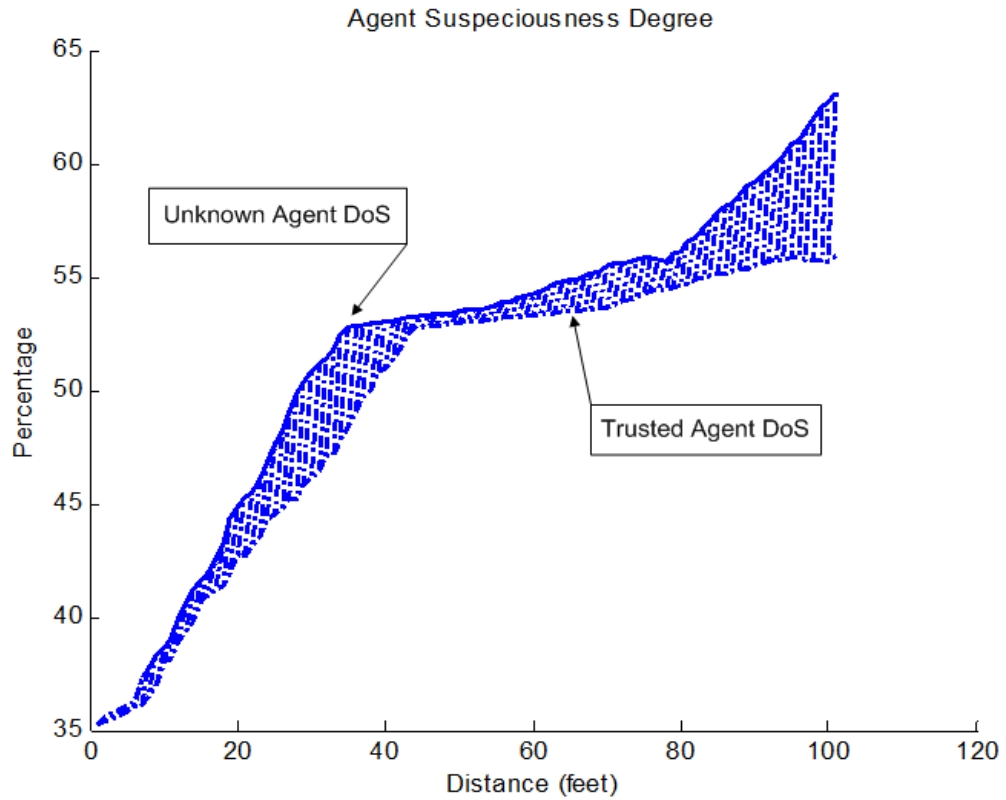


Figure 16. Agent suspiciousness degree as it moves

## VIII. CONCLUSION AND FUTRUE WORK

Applying sensor similarity and complementarity (homogeneous and heterogeneous) concepts that are developed in this paper and helped improving the performance of a dynamic security monitoring system as they handled processing similar and different data types of multiple sensors. With Kalman filter and interval type-2 fuzzy inference help, the system was able to predict agent's next position and report its security status. The proposed system exhibits promising performance in security monitoring and agent security status evaluation.

One future system improvement is to introduce relationship between multiple agents.

## ACKNOWLEDGEMENT

Authors would like to thank Prof. O. Castillo for providing us his own made type-2 fuzzy toolbox [20], his help is much appreciated.

## REFERENCES

- [1] M. Zohdy, A. Khan, "Global Optimization of Stochastic Multivariable Functions": American Control Conference, pp. 2339, 1993.
- [2] H. Hujun and Z. Yaning, "Multi-source Data Fusion Technology and Its Application in Geological and Mineral Survey": Information Engineering and Computer Science (ICIECS), 2010 2nd International Conference, pp. 1-6, 2010.
- [3] D. L. Hall and J. Llinas, "An Introduction to Multisensor Data Fusion": Circuits and Systems, ISCAS '98. Proceedings of the 1998 IEEE International Symposium on, pp. 537-540, 1998.
- [4] Q. Wu, D. Ferebee, Y. Lin and D. Dasgupta "An Integrated Cyber Security Monitoring System Using Correlation-based Techniques": System of Systems Engineering, 2009. SoSE 2009. IEEE International Conference, 2009.
- [5] R. Tenney and N. Sandell, "Detection with distributed sensors,": IEEE Trans. Aerospace and Electronic Systems, vol. AES-17, pp. 501-510, July 1981.

- [6] T. Dakhllallah, M. Zohdy and O. Salim, "Application of Hyper-Fuzzy Logic Decisions for A Security Monitoring System,": 2011 3<sup>rd</sup> International Conference on Computer and Automation Engineering (ICCAE 2011), pp. V1-387, 2011.
- [7] LV-MaxSonar®-EZ0™ High Performance Sonar Range Finder. MaxBotix, MaxSonar & EZ0 are trademarks of MaxBotix Inc. 2005.
- [8] CSI 430 SpeedVue™ Laser Speed Sensor. Emerson Process Management.2009.
- [9] MiniVLS nL Series Optical Speed/ Phase Sensors VLS nL, Compact Instruments.
- [10] Tag-it HF-I Standard, 13.56 MHZ, Transponder Inlays, ISO/IEC 15693 and ISO/IEC 18000-3 global open standards, Texas Instruments, 2005.
- [11] Smart card SCC-3, 3.125khz+UHF EPC GEN2, Rui Yue RFID Co., LTD., 2006.
- [12] Albert Leon-Garcia, 'Probability and Random Processes for Electrical Engineering', 2nd Edition, Pearson/Prentice Hall (2008) .
- [13] V. Subramanian, T. F. Burks and W. E. Dixon, "Sensor Fusion Using Fuzzy Logic Enhanced Kalman Filter For Autonomous Vehicle Guidance In Citrus Groves", transaction of ASABE (American Society of Agricultural and Biological Engineers), vol 52(5), 2009.
- [14] G. Welch, G. Bishop, "An Introduction to the Kalman Filter,," University of North Carolina at Chapel Hill Department of Computer Science, 2001.
- [15] R. C. Luo and C. Yih, "Multisensor Fusion and Integration: Approaches, Applications and Future Research Directories". Department of Electrical Engineering, National Chung Cheng University. IEEE Sensors Journal, Vol. 2, No. 2, 2002.
- [16] O. Castillo, P. Mellin, 'Type-2 Fuzzy Logic: Theory and Applications', Tijuana Institute of Technology, Division of Graduate Studies., vol.223, 2008.
- [17] Q. Liang and J. Mendel, "Interval Type-2 Fuzzy Logic Systems: Theory and Design": IEEE TRANSACTIONS ON FUZZY SYSTEMS, VOL. 8, NO. 5, OCTOBER 2000.
- [18] J. Mendel, 'Uncertain Rule-based fuzzy logic systems: Introduction and New Directions', NJ: Prentice-Hall, 2001.
- [19] H. Youpeng, L. Lin and Z. Yongfeng ; "A Hetrogenous Sensors Track-to-Track Correlation Algorithm Based on Fuzzy Numbers Similarity Degree": Information and Computing Science, 2009. ICIC '09. Second International Conference, pp. 191, 2009.
- [20] J. R. Castro, O. Castillo and P. Melin, "An Interval Type-2 Fuzzy Logic Toolbox for Control Applications,": International Conference on Fuzzy Systems, pp. 1-6, 2007.